

Regional characterization of ENSO effects on the seasonal rainfall of Sinaloa, Mexico

César Enrique ROMERO HIGAREDA, Bladimir SALOMÓN MONTIJO*, Juana CÁZARES MARTÍNEZ, José Saturnino DÍAZ and José Miguel CORRALES SAUCEDA

Facultad de Biología, Universidad Autónoma de Sinaloa, Ciudad Universitaria, Blvd. Universitarios y Av. las Américas, 80013 Culiacán, Sinaloa, México.

*Corresponding author; email: vladimir.salomon@uas.edu.mx

Received: July 19, 2024; Accepted: November 12, 2024

RESUMEN

La estacionalidad de las precipitaciones que, entre otros factores, es determinada anualmente por el Monzón de Norteamérica, es de enorme relevancia para los ecosistemas áridos del noroeste de México. Un factor importante pero irregular que afecta la estacionalidad de las precipitaciones es El Niño-Oscilación del Sur (ENSO) y sus dos fases: El Niño y La Niña, las cuales pueden cambiar los patrones estacionales de precipitación. En este estudio, caracterizamos espacialmente los patrones estacionales de las precipitaciones de tres regiones fisiográficas de Sinaloa y estados adyacentes en el noroeste de México. Las covarianzas entre las fases de El Niño y La Niña y sus respectivas cantidades de precipitación de verano e invierno fueron estimadas regionalmente en cada estación. La magnitud de la covariación fue diferenciada entre regiones y caracterizada espacialmente. Se hizo un análisis multivariado para obtener una perspectiva simultánea de las variables asociadas a la precipitación. Se detectaron diferencias entre regiones para las variables asociadas a precipitación; la altitud y longitud explicaron la mayor parte de su variación espacial. La precipitación invernal se incrementó en todas las estaciones por El Niño y La Niña. El Niño redujo la precipitación en la mayoría de las estaciones en verano, La Niña incrementó la precipitación en verano. La covariación entre la precipitación de verano y El Niño y La Niña se diferenció entre regiones. La latitud y longitud se correlacionaron con la covariación entre El Niño y La Niña y la precipitación de invierno. La altitud se correlacionó con la interacción de la precipitación veraniega y El Niño y La Niña. El análisis multivariado segregó las regiones con base en la variación de la precipitación de invierno y anual, el número de eventos de precipitación y su estacionalidad.

ABSTRACT

Rainfall seasonality is of paramount relevance for the northwestern Mexican ecosystems. Among other factors, it is annually driven by the North American Monsoon. An outstanding yet irregular and changing factor that affects rainfall seasonality is the El Niño Southern Oscillation (ENSO) and its two phases, El Niño and La Niña, which can change the seasonal rainfall patterns. Here, we characterized spatially seasonal rainfall patterns of three physiographic regions of Sinaloa and adjacent states in northwestern Mexico. The covariances between El Niño and La Niña phases and their respective summer and winter rainfall amounts were estimated in each station within their regions. The magnitude of covariance was also differentiated among regions and characterized spatially. A multivariate analysis was performed to attain a simultaneous perspective of the rainfall-related variables. We detected differences among regions for the measured rainfall-related variables; altitude and longitude explained most of its spatial variation. Winter rainfall increased in all stations of El Niño and La Niña occurrence. El Niño decreased rainfall in most stations for summer, whilst La Niña increased rainfall in summer. Summer rainfall covariance with El Niño and La Niña was differentiated among regions. Latitude and longitude were correlated with the covariation between El Niño

and La Niña and winter rainfall. Altitude correlated to the interaction of summer rainfall and La Niña and El Niño. Multivariate analysis segregated regions on the variation of winter, annual rainfall, number of rainfall events, and rainfall seasonality.

Keywords: northwestern Mexico, seasonality, ENSO, geographic variation.

1. Introduction

Rainfall seasonality is a key feature of climate in many terrestrial ecosystems since it determines nearly all the environmental functions and responses through water availability. Therefore, rainfall seasonality becomes crucial in arid environments. It is relevant not only for ecosystemic responses but also for human primary economic activities, such as agriculture and cattle production.

Along the Pacific Mexican coast, the rainfall pattern is clearly seasonal. The main fraction of annual rainfall (APP) occurs mainly from June through early October as summer rainfall (SPP). Early SPP events are frequently the result of convective storms. In late summer, tropical storms, although being sporadic, significantly contribute to rainfall amounts via extreme precipitation events (Cavazos et al., 2008; Gutzler et al., 2013). Towards the northwest, the SPP fraction decreases whilst the winter rainfall (WPP) fraction increases until it becomes the larger fraction of APP in the extreme northwest Pacific coast of Mexico. WPP is associated with winter storms moving southwards and its interaction with humid tropical air coming from the Pacific Ocean heading northeast, colliding in the upper regions of the Sierra Madre Occidental (SMO).

The main factor driving the rainfall seasonality of northwest Mexico is the North American or Mexican Monsoon (NAM), which occurs from late June through September (Douglas et al., 1993; Gochis et al., 2006). This yearly process accumulates above 50 percent of the APP in Sinaloa. The NAM is shaped by complex interactions of several meteorological factors, which are thoroughly discussed by Hu and Feng (2002) and Vera et al. (2006), among others. An important spatial component of the SPP is the orographic effect created by the Sierra Madre (SM), which runs almost parallel to the coast but increases the distance from the shoreline moving north. The effect of topography in the development of convective rainfall is explained by Houze (2012) and,

specifically for this region, by Rowe et al. (2008) and Nesbitt et al. (2008).

An intercontinental-scale phenomenon that modifies the seasonal rainfall patterns in northwest Mexico is El Niño Southern Oscillation (ENSO) and its two phases: El Niño (warmer sea surface) and La Niña (colder sea surface). The teleconnections (i.e., effects) of ENSO on seasonal rainfall patterns are multifactorial and complex and often occur at a multicontinental scale, as described by Zhao et al. (2016), who, through data analysis and simulations, detected that heating in Eurasian non-monsoonal regions induced rainfall anomalies (reduction) in North America. Taschetto et al. (2020) described that during El Niño episodes, rainfall increased in southwest North America; also, in general terms, La Niña produced opposite conditions, but these were dependent on the location of the ENSO anomaly plus the interaction of ENSO variation in different oceanic basins and non-equatorial regions. Rodríguez-Morales et al. (2023) detected divergent effects of the Atlantic Multidecadal Oscillation (AMO) and ENSO variation. The nature of these effects was also differentiated by regions on the Mexican coast. Llanes-Cárdenas et al. (2020) depicted a positive correlation between the Pacific Decadal Oscillation (PDO) and El Niño for northwest Mexico, affecting extreme precipitation.

The effect of ENSO on seasonal rainfall amounts on the Pacific Mexican coast is dependent on the occurring phase (El Niño or La Niña), the season (winter or summer), and the region (north [above 22° N] or south). According to Magaña et al. (2003), Caso et al. (2007), and Bravo-Cabrera et al. (2010), rainfall amounts tend to decrease in winter in El Niño conditions in the southern portion of the Mexican Pacific coast; inversely, rainfall amounts increase in summer in the northern region. El Niño conditions reduce rainfall amounts in the South Pacific, whilst rainfall amounts remain with unnoticeable change in the North Pacific. As for La Niña, in winter in the

northern region, rainfall records were found to be lower; inversely, in the southern region, records were higher. In a yearly basis, La Niña tends to slightly increase rainfall amounts along the Pacific coast, although its signal is rather weak (Zermeño-Díaz and Gómez-Mendoza, 2023).

Most of the evidence detected for rainfall modification at small (local) scales is linked to anthropogenic processes such as deforestation. An essential issue regarding the connection between the loss of vegetal cover and the decrease in rainfall is spatial scale. Notaro and Gutzler (2012) found through simulations that the loss of vegetation cover could modify physical evapotranspiration processes, reducing water recycling and changing atmospheric dynamics, and finally reducing rainfall. Leite-Filho et al. (2021) detected from field data a strong correlation between forest loss and reduction of rainfall at larger scales of analysis, hence producing agricultural losses.

Seasonal rainfall patterns are key for ecosystem processes in arid environments such as those in northwest Mexico (Caso et al., 2007; Verduzco et al., 2015). Given the seasonal water availability, ENSO anomalies might alter ecological processes such as plant recruitment (Félix-Burrueal et al., 2021), primary productivity (Salinas-Zavala et al., 2002), tree growth

(Pompa-García et al., 2014), and animal ecology (Mandujano, 2006).

Sinaloa and southern Sonora are the main agricultural regions in Mexico, whose crop production is dependent on the water availability of rivers that flow westward. Therefore, ENSO anomalies might constitute a factor that modifies crop yield and volume (Muñoz-Arriola et al., 2009; Cruz-González et al., 2024).

1.1 Sinaloa and its regions

Sinaloa is located in northwest Mexico. Together with the southwestern tip of the state of Chihuahua, the southern edge of Sonora and the eastern slopes of Durango, it is part of the Pacific northwest watershed, as delineated by the Comisión Nacional del Agua (National Water Commission, CNA). Essentially based on elevation, three main physiographic regions make up the state of Sinaloa within the watershed: the Coastal Plains (CP), situated along the Pacific coastline, with increasing width towards the northwest of the state; the low elevations of the Sierra foothills (SF), initially scattered, moving east with increasing altitude; and, finally, the SMO, the easternmost region, which runs almost parallel to the Pacific coasts and where all the state's rivers originate (Fig. 1).

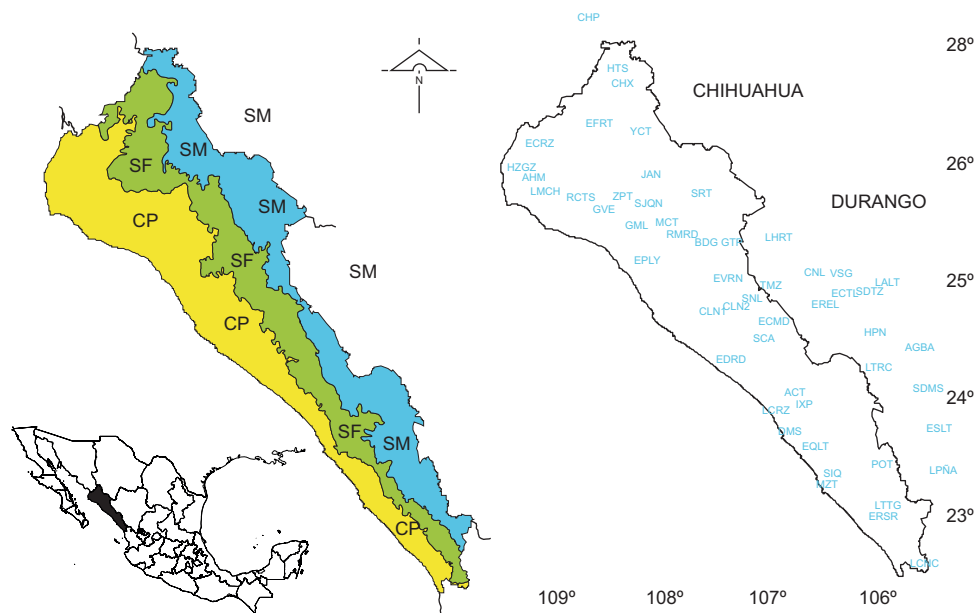


Fig. 1. Left panel: Sinaloa in northwest Mexico and its physiographic regions. Right panel: location of the climate stations. CP: coastal plains (yellow); SF: Sierra foothills (green); SM: Sierra Madre (blue).

Given the relevance of the rainfall seasonality patterns for this region and the potential effect of ENSO-driven anomalies, the objectives of this analysis were to: (1) characterize the covariance of the seasonal winter-summer rainfall related variables and geographic factors; (2) quantify the covariance between El Niño/La Niña values in each station, with their respective amounts of winter-summer rainfall; (3) estimate regional differences of the quantified covariance magnitude values of El Niño/La Niña-seasonal rainfall amounts; (4) determine the correlation of the quantified covariance of El Niño/La Niña-seasonal rainfall with geographic elements, and (5) describe the variation of seasonal rainfall-related variables from a multivariate perspective.

Caso et al. (2007) stated that along the Mexican Pacific northwest coast, there is a decrease in mean annual rainfall and summer means decrease, while winter rainfall increases towards the north. Annual and summer rainfall are expected to increase altitudinally by the orographic effect in convective rainfall, as described by Nesbitt et al. (2008) and Rowe et al. (2008). These trends have yet to be quantified for the state of Sinaloa. In addition, we also estimated another related seasonal rainfall variable. Likewise, we incorporated longitude to widen the perspective of spatial analysis.

2. Materials and methods

2.1 Climate data

From the records of the Servicio Meteorológico Nacional (National Weather Service, SMN)-CNA website, based on its entirety, we chose and downloaded daily data from 53 stations (Table I). Data from the selected stations was updated through 2022 by the CNA regional office. From every selected station, we calculated monthly totals for each recorded year. We also considered stations in the states of Chihuahua and Durango that belong to the same regional North Pacific watershed since the rivers that flow into Sinaloa originate from these sites.

We settled the SPP season from May 15 to November, following the guidelines of the CNA that determine the major probabilities of hurricane occurrence on the Mexican Pacific coast for the period. Hence, the WPP season was delimited from December to May 14. We quantified the seasonal rainfall amounts as follows: WPP as the sum of monthly

rainfall from December to May 14 and SPP as the sum from May 15 to November. As an example, for any considered station here, the WPP of 1973 was the sum of December 1972 plus the totals of January, February, March, April, and the first 14 days of May of 1973; the 1973 SPP was considered as the total sum from the last 16 days of May to November, therefore, the APP amount of 1973 goes from December 1972 to November 1973.

For the analysis, in addition to APP, SPP, and WPP, we included the percentage of WPP calculated as

$$\%WPP = (WPP/APP) \times 100 \quad (1)$$

We also included the mean number of rainfall events per year (PPE), estimated from daily rainfall data provided by the CNA. Finally, we incorporated the precipitation concentration index (PCI) proposed by Oliver (1980) for an annual scale proposed, estimated as:

$$PCI = \frac{\sum p_i^2}{(\sum p_i)^2} \cdot 100 \quad (2)$$

where the numerator is the sum of squared monthly rainfall amounts, and the denominator is the squared total annual rainfall amount. This measure of annual rainfall variation indicates that larger values describe a higher level of rainfall seasonality, e.g., a larger amount of annual rainfall in fewer months.

Monthly Oceanic Niño Index values were obtained from the NWS Climate Prediction Center webpage (ONI, n.d.). These values are estimated as a three-month rolling average temperature difference of sea surface temperature in the tropical eastern Pacific. Values of 0.5 or above point to El Niño conditions; values of -0.5 or below indicate La Niña conditions.

2.2 Data analysis

We explored the covariance of the stations' APP, SPP, WPP, and %WPP means with latitude, longitude, and altitude by linear regression analysis. We chose these geographic elements due to their accessibility and ease of interpretation.

To elucidate the effect of ENSO variation on seasonal rainfall amounts, we separated monthly ONI data values for El Niño (warm) and La Niña (cold)

Table I. Selected stations from three regions in northwestern Mexico (n = 53).

Name and 1st year of data	Abbreviation	Region	Latitude	Longitude	Altitude (masl)	APP	WPP	%WPP	PPE	PCI
Acatitán (1962)	ACT	SF	24° 05'	−106° 40'	96	787.1	64.3	8.10	64	24.4
Agua Blanca (1981)	AGBA	SM	24° 26'	−105° 47'	2500	1202.5	56.8	9.23	101	18.4
Ahome (1962)	AHM	CP	25° 55'	−111° 52'	10	363.4	53.5	15.0	30	29.6
Badiraguato (1961)	BDG	SF	25° 20'	−107° 32'	190	951.4	71.3	7.17	60	25.3
Canelas (1961)	CNL	SF	25° 07'	−106° 32'	1754	1300.9	178.4	12.8	101	19.8
Chinipas (1961)	CHP	SF	27° 23'	−108° 32'	440	747.9	108.1	13.7	66	21.9
Choix (1961)	CHX	SF	26° 42'	−108° 19'	240	770.5	101.9	12.6	61	22.1
Culiacán_CNA (1961)	CLN1	CP	24° 48'	−107° 24'	40	678.5	59.6	8.55	55	27.8
Culiacán_UAS (1995)	CLN2	CP	24° 49'	−107° 22'	62	701.5	33.9	5.16	61	28.8
Dimas (1962)	DMS	CP	23° 43'	−106° 46'	20	574.2	53.1	11.1	31	30.0
El Cantil (1961)	ECTL	SM	24° 56'	−106° 15'	2240	1468.5	216.4	14.0	95	19.6
El Carrizo (1969)	ECRZ	CP	26° 16'	−109° 02'	9	361.5	51.8	13.9	34	27.1
El Comedero (1981)	ECMD	SF	24° 37'	−106° 48'	311	973.6	66.9	6.83	56	25.1
El Dorado (1970)	EDRD	CP	24° 19'	−107° 22'	12	445.4	27.6	6.72	39	29.4
El Fuerte (1961)	EFRT	SF	26° 24'	−108° 37'	86	597.6	70.7	10.9	50	27.8
El Playón (1962)	EPLY	CP	25° 13'	−108° 11'	6	477.4	46.7	9.89	51	25.5
El Quelite (1961)	EQLT	CP	23° 33'	−106° 27'	49	613.6	53.1	8.53	51	25.5
El Real (1978)	EREL	SF	24° 42'	−106° 32'	457	757.2	125.9	14.9	71	21.1
El Rosario (1963)	ERSR	CP	22° 59'	−105° 51'	32	917.6	54.7	5.79	59	25.8
El Salto (1961)	ESLT	SM	23° 41'	−105° 21'	2538	979.4	148.4	14.2	90	18.1
El Varejonal (1961)	EVRN	SF	25° 05'	−107° 23'	120	897.3	79.3	8.63	55	25.4
Guamúchil (1961)	GML	CP	25° 28'	−108° 11'	44	554.9	46.1	8.86	53	26.4
Guasave (1969)	GVE	CP	25° 33'	−108° 27'	17	479.7	45.0	9.55	38	28.2
Guaténipa (1964)	GTP	SF	25° 20'	−107° 13'	293	798.7	164.1	18.9	73	18.0
Higuera de Zaragoza (1962)	HZGZ	CP	25° 58'	−109° 18'	10	318.9	49.7	14.9	25	30.8
Huahuapan (1967)	HPN	SM	24° 31'	−105° 57'	1170	808.4	101.2	12.1	84	19.5
Huites (1961)	HTS	SF	26° 53'	−108° 21'	260	707.2	104.0	12.4	53	22.6
Ixpalino (1961)	IXP	SF	23° 58'	−106° 36'	69	755.9	62.0	7.92	61	24.7
Jaina (1961)	JAN	SF	25° 53'	−108° 13'	261	868.6	79.4	9.11	65	24.2
La Concha (1961)	LCNC	CP	22° 31'	−105° 27'	16	1060.5	58.1	5.47	66	25.4
La Cruz (1969)	LCRZ	CP	23° 54'	−106° 54'	9	576.8	44.6	9.20	37	27.3
La Huerta (1969)	LHRT	SF	25° 21'	−106° 42'	670	787.9	169.9	19.4	73	17.8
La Peña (1963)	LPÑA	SM	23° 33'	−105° 24'	2756	1295.3	248.9	17.9	94	17.4
Las Tortugas (1974)	LTTG	SF	23° 05'	−105° 50'	65	895.7	46.8	5.08	61	25.5
Las Truchas (1962)	LTRC	SM	24° 10'	−105° 57'	1288	1260.5	186.0	14.2	110	18.7
Los Altares (1973)	LALT	SM	24° 59'	−105° 53'	2616	839.3	129.3	14.9	91	17.5
Los Mochis (1970)	LMCH	CP	25° 48'	−109° 02'	11	346.1	43.0	12.2	32.5	29.8
Mazatlán (1961)	MZT	CP	23° 12'	−106° 24'	4	796.2	30.9	4.14	49	27.7
Mocorito (1969)	MCT	SF	25° 28'	−107° 55'	87	706.3	63.5	8.94	54	26.7
Potrerrillos (1969)	POT	SM	23° 27'	−105° 49'	1572	1296.0	113.9	8.60	90	22.2
Rosa Morada (1962)	RMRD	SF	25° 21'	−107° 50'	134	782.1	57.4	7.14	47.1	27.0
Ruiz Cortines (1963)	RCTS	CP	25° 42'	−108° 43'	20	416.2	42.2	9.91	32.3	28.7
San Diego (1973)	SDTZ	SM	24° 53'	−106° 07'	1640	807.0	101.2	11.9	85	19.9
San Joaquín (1979)	SJQN	SF	25° 40'	−108° 01'	144	758.9	58.5	7.11	49	27.4
Sanalona (1961)	SNL	SF	24° 48'	107° 09'	104	861.5	63.3	7.45	63	25.6
Santa Cruz (1961)	SCA	SF	24° 29'	−106° 57'	109	771.8	74.6	9.39	64	25.0
San Dimas (1962)	SDMS	SM	24° 08'	−105° 35'	952	901.6	114.9	12.4	80	20.4
Siqueros (1961)	SIQ	CP	23° 20'	−106° 14'	40	743.5	52.2	6.77	56	25.8
Surutato (1961)	SRT	SM	25° 48'	−107° 33'	1460	1190.1	195.4	15.2	90	19.1
Tamazula (1961)	TMZ	SF	24° 58'	−106° 58'	264	1001.2	94.0	8.82	75	23.9
Vasco Gil (1967)	VSG	SM	25° 07'	−106° 21'	2400	1314.4	274.8	19.4	132	16.5
Yecorato (1967)	YCT	SF	26° 25'	−108° 13'	400	802.0	104.9	12.5	59	22.4
Zopilote (1979)	ZPT	CP	25° 43'	−108° 20'	37	565.3	37.8	6.36	36	29.4

APP: annual rainfall (mm); WPP: winter rainfall (mm); %WPP: percentage of winter rainfall; PPE: rainfall events; PCI: precipitation concentration index.

conditions. Then we performed four non-parametric Spearman correlation (ρ) analyses ($P < 0.05$) on each selected station: (1) between the ONI monthly data set of El Niño and its corresponding WPP amount; (2) between El Niño and its respective SPP amount; (3) we repeated the process between La Niña and WPP, and (4) La Niña and SPP amounts. We selected Spearman's ρ correlation since monthly seasonal rainfall data in most of the stations were not normally distributed and/or lacked homogeneity of variance. To assess differences among regions of the quantified magnitude of Spearman's (ρ) coefficients, we performed a one-way ANOVA ($P < 0.05$).

To explore the covariance of the quantified Spearman's ρ products of El Niño/La Niña and seasonal rainfall in terms of geographic variation, a linear regression of their magnitudes was performed with values of latitude, longitude, and altitude. Also, a spatial autocorrelation analysis was carried out using Moran's I index for the Spearman's ρ products quantified from the correlations between El Niño/La Niña ONI and WPP-SPP.

Finally, a principal component analysis was performed to achieve a simultaneous perspective of the total variation of the seasonal rainfall variables assessed plus the effect of ENSO on the seasonal rainfall. We used an Oblimin oblique rotation since the considered variables were highly correlated.

3. Results

3.1 Annual and seasonal rainfall

An initial descriptive analysis of the rainfall-related variables showed that the SM, APP, and SPP means

almost double the CP mean. The WPP mean is almost four times larger in the SM as compared to CP (Table II). %WPP is also the largest in the SM, while there were no significant differences between the CP and the SF regions. The number of PPE in the CP is half of the mean value detected in the SM region. The highest seasonality for the rainfall regime was detected for CP.

The regression analysis with the geographic features of the sampled stations showed that APP and SPP had negative correlations with latitude and positive correlations with longitude and altitude. So, their means were smaller towards the north, the west, and higher sites. WPP and %WPP showed higher means in northern and higher sites; in contrast, WPP means were lower in western stations, while %WPP values were higher. PPE correlated negatively with latitude and positively with longitude and altitude, exactly the opposite pattern than PCI (Table III).

3.2 El Niño and La Niña effects on seasonal rainfall

The effect of El Niño conditions on the WPP amounts indicated that positive correlations occurred in all the stations, hence increasing rainfall. Only in Rosa Morada, Huahuapan, and Culiacán-UAS were the results statistically non-significant (Fig. 2a). The magnitude of Spearman's ρ ranged from 0.463 in Acatitán to 0.150 in Mocorito. Contrastingly, in El Niño conditions with SPP (Fig. 2b), 45 stations produced negative correlations, pointing to a reduction in rainfall. Eight stations had positive correlations (yellow squares in Fig. 2) that were non-significant, most of them in the CP region. Larger intensities were detected in the SF and SM regions.

Table II. Means \pm S.E. of annual rainfall, percentage of winter rainfall, annual rainfall events, and precipitation concentration index of 53 stations from three regions in northwestern Mexico.

	Coastal plains	Sierra foothills	Sierra Madre
Annual rainfall (mm)	578.5 \pm 46.1 ^c	817.4 \pm 20.0 ^b	1152.0 \pm 67.0 ^a
Summer rainfall (mm)	532.0 \pm 45.8 ^c	728.9 \pm 21.6 ^b	989.4 \pm 58.0 ^a
Winter rainfall (mm)	46.5 \pm 2.1 ^c	88.46 \pm 7.1 ^b	162.6 \pm 18.9 ^a
% winter rainfall	9.05 \pm 0.74 ^b	10.42 \pm 0.81 ^b	13.71 \pm 0.90 ^a
Rainfall events	42.8 \pm 2.91 ^c	61.9 \pm 1.86 ^b	97.1 \pm 3.84 ^a
Precipitation concentration index	27.9 \pm 0.37 ^a	23.7 \pm 0.56 ^b	18.9 \pm 0.43 ^c

Superscript letters denote Tukey post hoc differences: a > b > c.

Table III. Regression coefficients (R^2), slope, and statistical significance ($P < 0.05$) of rainfall-related variables in 53 meteorological stations of the North Pacific watershed in northwestern Mexico.

Variable	Latitude (N)			Longitude (W)			Altitude (m)		
	R^2	Slope	P	R^2	Slope	P	R^2	Slope	P
APP	0.100	-81.09	0.021	0.466	170.6	0.000	0.513	0.231	0.000
SPP	0.143	-83.48	0.005	0.487	150.3	0.000	0.415	0.180	0.000
WPP	0.002	2.392	0.750	0.151	20.33	0.004	0.593	0.052	0.000
%WPP	0.134	1.308	0.007	0.001	-0.115	0.815	0.282	0.002	0.000
PPE	0.046	-4.647	0.124	0.459	14.32	0.000	0.715	0.023	0.000
PCI	0.003	0.193	0.713	0.336	-2.104	0.000	0.663	-0.004	0.000

APP: annual rainfall; SPP: summer rainfall; WPP: winter rainfall; %WPP: percentage of winter rainfall; PPE: annual rainfall events; PCI: precipitation concentration index.

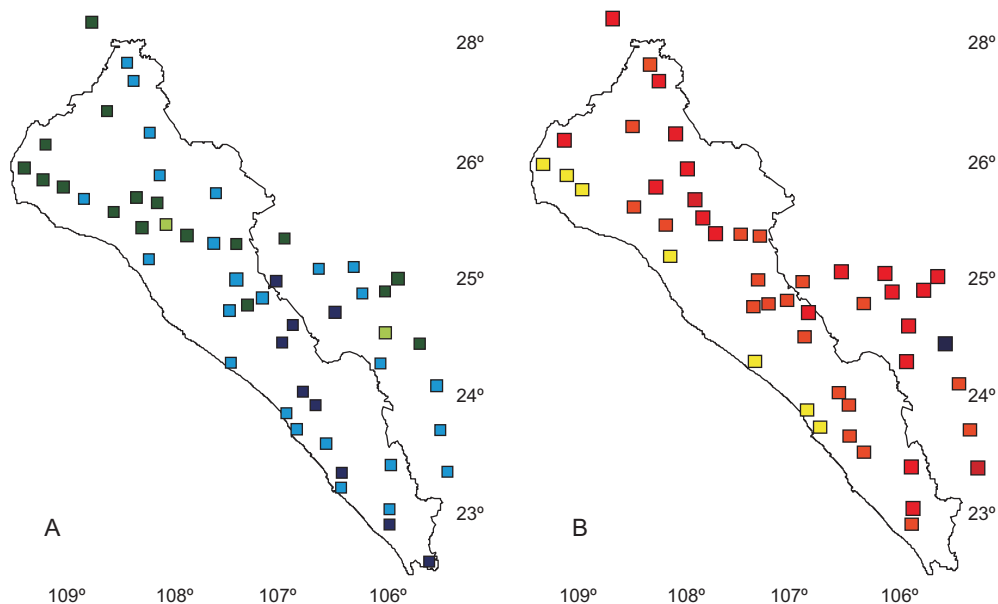


Fig. 2. Spearman's ρ correlations analysis between El Niño ONI values and (a) winter rainfall amounts and (b) summer rainfall amounts in 53 stations of the North Pacific watershed of northwestern Mexico. Magnitudes of Spearman's ρ correlations: blue (■): 0.499 to 0.400; cyan (■): 0.399 to 0.300; green (■): 0.299 to 0.200; olive green (■): 0.199 to 0.100; yellow (■): 0.099 to 0.0; orange (■): -0.001 to -0.100; red (■): -0.101 to -0.200; purple (■): -0.201 to -0.360.

Spearman's ρ correlation magnitudes between La Niña ONI values and WPP amounts ranged from 0.200 in Acatitán to -0.115 in Rosa Morada; also, Chinipas, El Carrizo, Mocorito, and Yecorato showed negative signs in such correlations (Fig. 3a). The correlations products between La Niña ONI values and SPP amounts were all positive in the studied stations, hence describing increasing rainfall amounts. The SF

and SM regions showed larger magnitudes of these correlation products (Fig. 3b).

3.3 Regional differences of Spearman's ρ magnitude

We found a normal distribution of Spearman's ρ magnitude for each analysis, and hence, we performed a one-way ANOVA between regions. Overall, the

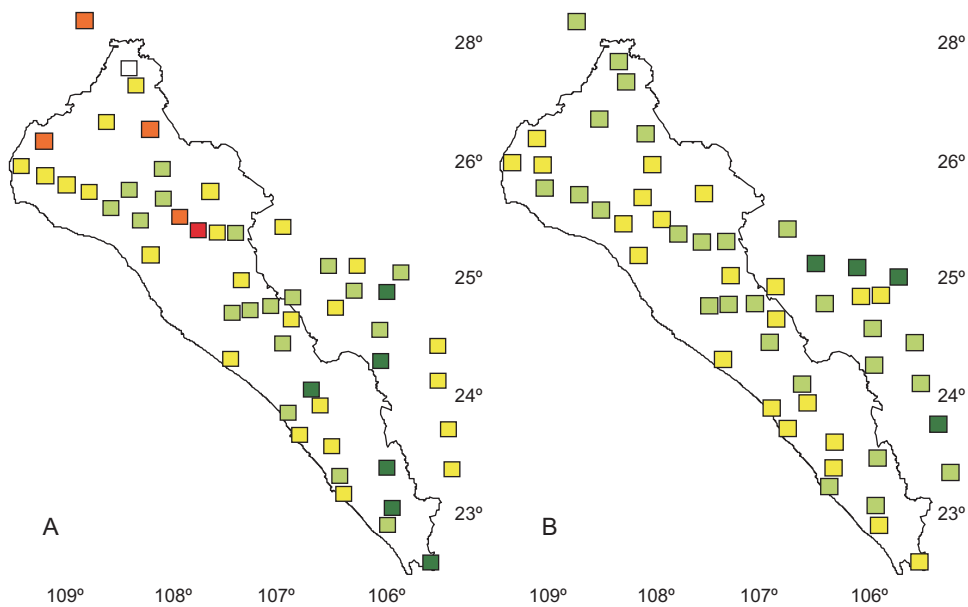


Fig. 3. Spearman's ρ correlations analysis between La Niña ONI values and (a) winter rainfall amounts and (b) summer rainfall amounts in 53 stations of the North Pacific watershed of northwestern Mexico. Magnitudes of Spearman's ρ correlations: blue (■): 0.499 to 0.400; cyan (■): 0.399 to 0.300; green (■): 0.299 to 0.200; olive green (■): 0.199 to 0.100; yellow (■): 0.099 to 0.0; orange (■): -0.001 to -0.100; red (■): -0.101 to -0.200; purple (■): -0.201 to -0.360.

largest mean value was found in El Niño-WPP, and the minimum mean was detected in La Niña-WPP; however, both winter interactions were not regionally differentiated. On the other hand, summer rainfall was differentiated in the direction of the mean correlations; they were negative in El Niño (reducing rainfall) and positive during La Niña (increasing rainfall). Both summer season rainfall correlations with El Niño/La Niña were different between regions, where the SM magnitudes were always larger (Table IV).

3.4 Geographic and spatial covariation of ENSO rainfall amounts

Latitude correlates significantly with Spearman's ρ coefficients of El Niño-WPP (Fig. 4a) and La Niña-SPP (Fig. 4b), with smaller coefficients toward the north in both cases.

Longitude generated three significant regressions with Spearman's ρ values: El Niño-WPP, El Niño-SPP, and La Niña-WPP (Fig. 5).

Altitude produced two significant regressions with Spearman's ρ values: El Niño-SPP correlated

Table IV. Mean Spearman's ρ values (\pm S.E.) of the covariance between El Niño and La Niña phases and winter and summer rainfall amounts for 53 stations of three physiographic regions in the North Pacific watershed of Mexico.

ENSO-seasonal rainfall	Coastal plains	Sierra foothills	Sierra Madre	Overall
El Niño-winter	0.320 ± 0.014	0.341 ± 0.017	0.315 ± 0.018	0.328 ± 0.010
El Niño-summer	-0.025 ± 0.015^a	-0.091 ± 0.011^b	-0.137 ± 0.019^b	-0.078 ± 0.010
La Niña-winter	0.096 ± 0.015	0.076 ± 0.018	0.135 ± 0.018	0.097 ± 0.010
La Niña-summer	0.077 ± 0.012^b	0.112 ± 0.007^{ab}	0.141 ± 0.015^a	0.106 ± 0.007

Superscript letters denote Tukey post hoc differences: $a > b > c$.

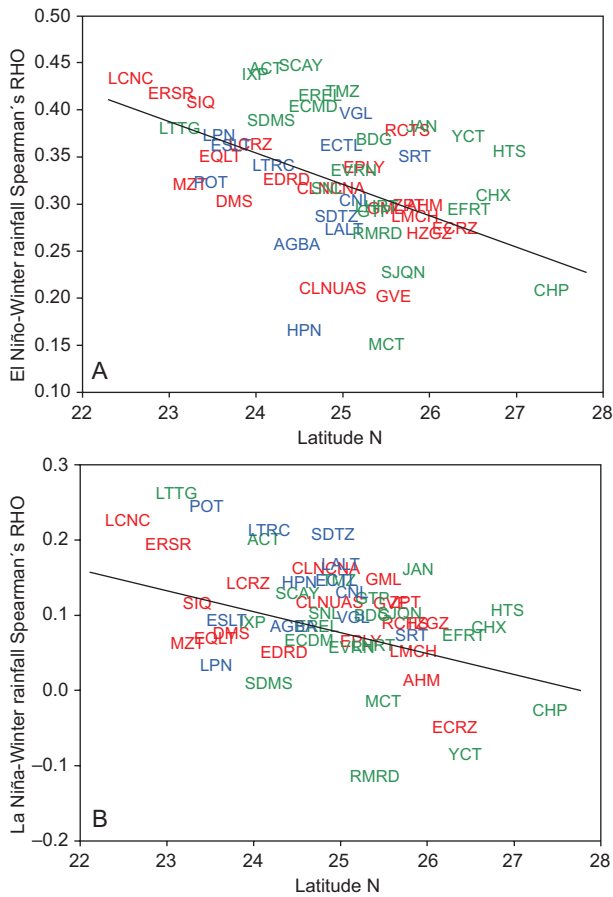


Fig. 4. Regression analysis of 53 stations within three physiographic regions in northwestern Mexico. (a) latitude and El Niño-winter rainfall ($R^2 = 0.182$, $P < 0.001$, slope = -0.028); (b) latitude and La Niña-winter rainfall ($R^2 = 0.219$, $P < 0.000$, slope = -0.033). Red captions: coastal plains region; green captions: Sierra foothills region; blue captions: Sierra Madre region.

negatively with altitude (Fig. 6a), and La Niña-SPP coefficients correlated positively with altitude (Fig. 6b).

Two spatial Moran's I analyses were significant: El Niño-SPP: $I = 0.227$, $P < 0.001$, showing a clustered aggregation, and La Niña-SPP, which also developed a clustered aggregation: $I = 0.147$, $P < 0.028$.

3.5 Multivariate analysis

From a multivariate perspective, a principal component analysis (Table V) showed that the three first components explained over 80% of the total variation. PC1, which depicted 51%, was correlated

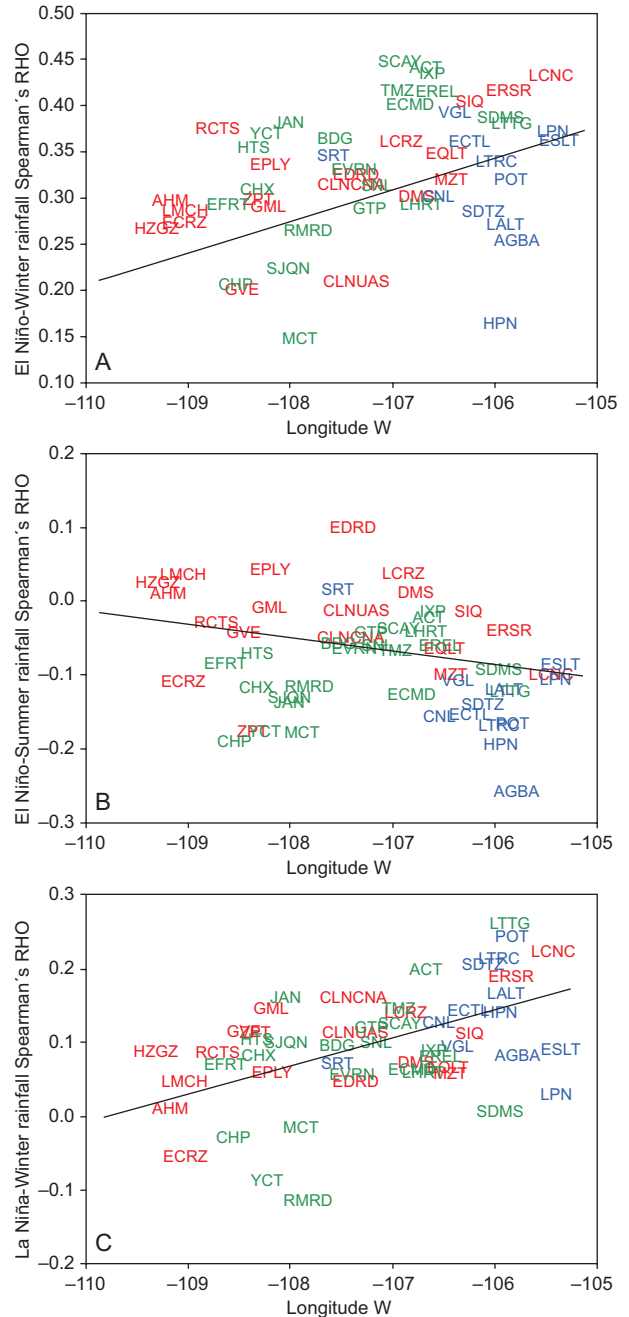


Fig. 5. Regression analysis of 53 stations within three physiographic regions in northwestern Mexico. (a) longitude and El Niño-winter rainfall ($R^2 = 0.129$, $P < 0.008$, slope = 0.023); (b) longitude and El Niño-summer rainfall ($R^2 = 0.077$, $P < 0.044$, slope = -0.033); (c) longitude and La Niña-winter rainfall ($R^2 = 0.222$, $P < 0.000$, slope = 0.032). Red captions: coastal plains region; green captions: Sierra foothills region; blue captions: Sierra Madre region.

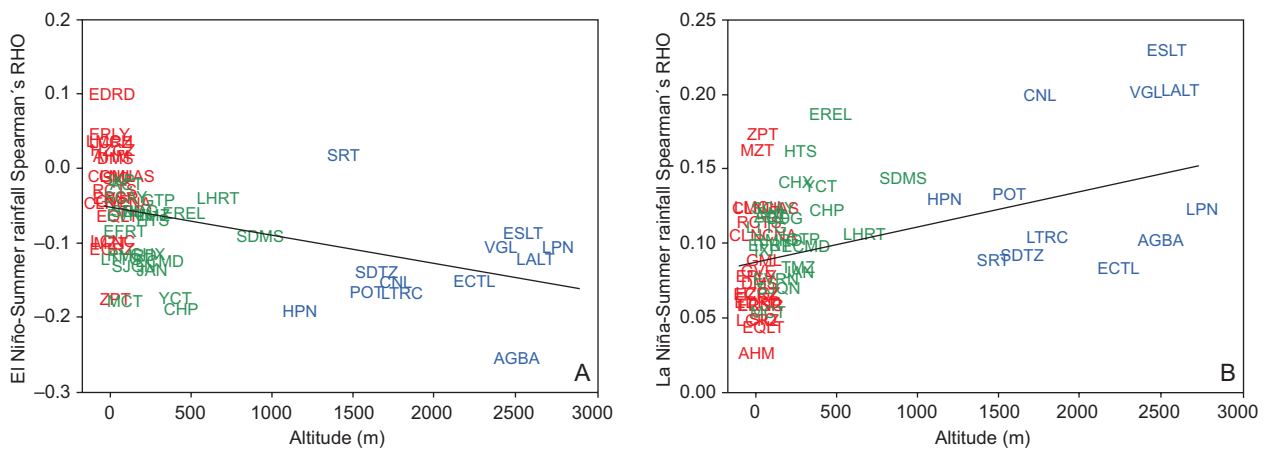


Fig. 6. Regression analysis of 53 stations within three physiographic regions in northwestern Mexico. (a) altitude and El Niño-summer rainfall ($R^2 = 0.220$, $P < 0.000$, slope = 4.03×10^{-5}); (b) altitude and La Niña-summer rainfall ($R^2 = 0.244$, $P < 0.000$, slope = 2.59×10^{-5}). Red captions: coastal plains region; green captions: Sierra foothills region; blue captions: Sierra Madre region.

Table V. Multivariate analysis (Oblimin rotation) loadings of Spearman's ρ coefficients from rainfall variables and ENSO phases (El Niño-La Niña), with winter and summer rainfall amounts of 53 stations from northwest Mexico. Loadings above 0.300 in boldface.

	PC1	PC2	PC3
Explained variance (%)	50.57	17.40	12.42
Accumulated variance (%)	—	67.97	80.39
Annual rainfall	0.669	0.676	-0.619
Summer rainfall	0.543	0.725	-0.661
Winter rainfall	0.962	0.243	-0.234
% winter rainfall	0.808	-0.280	0.132
Rainfall events	0.830	0.506	-0.570
Precipitation Concentration Index	-0.918	-0.300	0.444
El Niño-Winter rainfall	0.111	0.717	0.361
El Niño-Summer rainfall	-0.351	-0.072	0.914
La Niña-Winter rainfall	-0.021	0.719	-0.125
La Niña-Summer rainfall	0.555	0.111	-0.328

Bold letters: loadings above 0.300.

positively with WPP, the number of rainfall events, the percentage of WPP, APP, and the covariance of La Niña-SPP and SPP. The largest negative loadings of PC1 were the PCI and El Niño-SPP. PC2 illustrated 17% of the total variation; here, the main positive loadings were SPP, the covariance of La Niña-WPP, El Niño-WPP, APP, and a number of rainfall events; the largest negative loading was the PCI. The main positive loadings in PC3 were the covariances of El

Niño-SPP and El Niño-WPP plus the PCI; the largest negative loadings were SPP, APP, the number of rainfall events, and the La Niña-SPP relationship.

A graphic analysis of the z-standardized scores for PC1 and PC2 (Fig. 7) calculated from the multivariate analysis, depicted that on the negative sector of PC1, the variability of all CP stations plus Acatitán, Badiraguato, El Comedero, El Fuerte, El Varejonal, Ixpallino, Jaina, Las Tortugas, Mocorito,

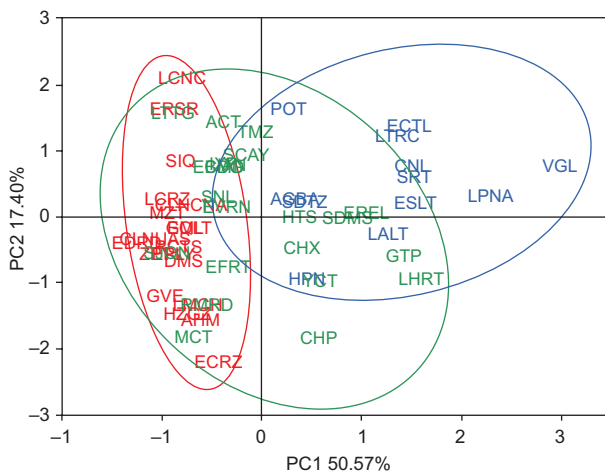


Fig. 7. Scatter plot of z-scores of principal component analysis for rainfall variables and the effect of El Niño and La Niña conditions on seasonal rainfall of 53 stations from three regions of the North Pacific watershed in northwestern Mexico. Red captions: coastal plains region; green captions: Sierra foothills region; blue captions: Sierra Madre region.

Rosa Morada, San Joaquín, Sanalona, Santa Cruz, and Tamazula from the SF region, was determined by high values of PCI and the correlation of El Niño-SPP. In the positive sector of PC2, all the stations of the SM region besides Huities, San Dimas, El Real, Choix, Chinipas, Guaténipa, and La Huerta from the SF region were linked to high means of APP, SPP, WPP, %WPP, number of rainfall events, and the correlation of La Niña-SPP.

4. Discussion

4.1 Rainfall and geography

In the scenario described by Caso et al. (2007), the state of Sinaloa is located at the northern end of a summer-rainfall regime along the transition summer-to-winter rainfall dominance on the Pacific coast of Mexico. Here, regional differences within the Pacific Northwest watershed for all the rainfall-related variables indicated that rainfall seasonal patterns are differentiated. These differences were correlated to geographical variations: the APP mean values decrease heading north and west; APP and SPP clearly decrease into the lower altitudes of the CP, an effect described by Houze et al. (2012), and

WPP and %WPP increase toward the north and in upper stations. In addition, in the northwest and lowlands, there is a decreasing gradient of PPE and an increasing trend in the values of %WPP and rainfall seasonality (PCI).

4.2 Effects of El Niño and La Niña on seasonal rainfall and regional differences

Regarding the ENSO covariance with seasonal rainfall in Sinaloa during winter, El Niño increased rainfall amounts in each studied station as described by Magaña et al. (2003), Caso et al. (2007), and Bravo-Cabrera et al. (2010). The magnitude of El Niño's effect in each region is similar, with over 30% of explained covariance. On the contrary, in summer, with El Niño warm-ocean conditions, rainfall in Sinaloa developed a similar pattern as in the southern regions of the Mexican Pacific coasts, with 85% of the studied stations recording decreasing rainfall amount trends. Among regions, the SF and the SM showed the largest negative mean correlations, pointing that in these conditions, El Niño may decrease water availability during the summer, thus disrupting or delaying ecosystemic processes.

In reference to La Niña, our results also coincide with those of Magaña et al. (2003), Caso et al. (2007) and Bravo-Cabrera et al. (2010) for the WPP and SPP regimes, for which they depicted slightly increasing trends in both seasons. The effect of La Niña and WPP in Sinaloa showed mostly increasing rainfall trends. The magnitude of the overall Spearman's ρ in each of the analyzed regions was the lowest, in accordance with the analysis of Zermeño-Díaz and Gómez-Mendoza (2023), who depicted a weak signal of the La Niña-WPP for northwestern Mexico. As for the covariation of La Niña and the SPP, all the analyzed stations in Sinaloa developed increasing trends. Here, the detected differences among regions showed a larger effect on the SM and SM foothills regions. This scenario could potentially mitigate dryness in the seasonal regions by increasing rainfall and/or advancing the start of the rainy season.

A relevant feature of the spatial distribution of the covariances of ENSO variation on the seasonal rainfall amounts is its homogeneity. In the four performed analyses, we did not detect relevant spatial discrepancies in the directions of correlations in nearby stations. These results suggest that spatial physical

heterogeneity does affect local rainfall regimes under ENSO variation, although further research needs to be done in this area.

4.3 Geographic and spatial covariance

Although El Niño and La Niña physical conditions are opposed, their Spearman's ρ correlation products with WPP amounts correlated in the same manner with latitude. These two results, together with those described by regression between longitude-El Niño-WPP and longitude-La Niña-WPP, indicate that rainfall amounts in the southern and eastern stations of the studied area are prone to increase during winter in both extremes of the ENSO variation. In contrast, as depicted by the regression between longitude and El Niño-SPP, southeastern stations are more sensitive to Pacific warmer water conditions; in this case, although these stations possess larger SPP means in such scenario, rainfall below its average would enhance lack of water availability and so dry conditions during summer due to frequent elevated temperatures in such season.

Regarding altitude, summer rainfall regressions generated two contrasting directions. During El Niño conditions, a few CP stations plus Surutato from the SM region tend to develop a minor increase in rainfall amounts. This condition could slightly mitigate dry conditions in that region, but the SF and the SM stations developed negative trends. Hence, in such regions is evident that El Niño decreases water availability in summer. On the contrary, during La Niña in summer, as altitude increases across regions, the covariation of La Niña and rainfall amounts increases accordingly, hence ameliorating dry conditions due to increased rainfall conditions in all stations.

4.4 Multivariate analysis

From a multivariate perspective, the relevance of ENSO variations in seasonal rainfall amounts seems rather scarce, given the explained variance of the principal components. In PC1, which explains half of the total variance, most of the variation is illustrated by the weights of APP, SPP, WPP, %WPP, number of rainfall events, and PCI. Nevertheless, correlations of El Niño-SPP and La Niña-SPP found in PC1 are important. El Niño-SPP correlation and PCI mainly determine the multivariate responses of CP and 14 stations of the SF, indicating that summer rainfall

would increase in this area if El Niño is present. On the other hand, if La Niña is present in summer, rainfall amounts would increase in all SM and eight stations of the SF.

For PC2, El Niño-WPP and La Niña-WPP are relevant in 10 of the 12 stations of the SM region, southern CP stations, and 10 SF stations. This depicts that in winter, regardless of the contrasting El Niño and La Niña conditions, rainfall amounts could increase in the aforementioned stations.

5. Conclusions

All the seasonal rainfall variables analyzed here were differentiated on a regional scale. Altitude was correlated significantly to all seasonal rainfall variables, pointing to the relevance of orography in the development of rainfall convective processes for the SF and SM stations. Although there is a decrease in APP, SPP, and WPP means towards the north and lower altitudes, the %WPP increases. This percentage of water is of paramount relevance for ecosystem processes since it can mitigate the lack of humidity during the following dry season. Contrary to expectations, longitude presented twice as many significant results as latitude.

The effect of ENSO in seasonal rainfall amounts in the analyzed watershed is better described by seasons. In winter, the effect of El Niño tends to be more homogeneous in terms of direction by increasing chances of rainfall in all the studied stations, as depicted by the regional non-significant differentiation. Similarly, although with less intensity, La Niña's effect in winter also increased rainfall amounts in Sinaloa and the rest of the watershed. Contrastingly, El Niño and La Niña showed opposite effects. El Niño showed negative correlations, pointing to decreasing rainfall amounts, whilst La Niña showed positive correlations (i.e., increasing rainfall) with a marked regional differentiation.

The effect of El Niño-SPP covariation in Sinaloa is particularly relevant since it is correlated to a decrease in rainfall amounts across all regions, potentially limiting water availability and worsening the effects of a prolonged dry season, hence affecting not only natural ecosystemic processes but also primary economic activities such as agriculture and cattle production.

Concerning the covariance of SPP with El Niño and La Niña, the regional differences in Spearman's ρ , linear regressions with longitude and altitude, and spatial Moran's autocorrelation obtained in this study suggest that summer seasonal rainfall in Sinaloa is highly reactive to both extremes of ENSO variation, producing opposite effects.

Latitudinally, regardless of the interaction with the contrasting conditions of El Niño/La Niña, the effects in the stations were very similar, with more notorious effects in southern stations. In terms of longitude, the correlation of WPP and El Niño/La Niña also occurred in the same manner as with larger effects towards eastern stations. On the contrary, SM stations showed a slightly more intense decrease in rainfall in the summer with El Niño conditions.

References

- Bravo-Cabrera JL, Azpra-Romero E, Zarraluqui-Such V, Gay-García C, Estrada Porrúa F. 2010. Significance tests for the relationship between “El Niño” phenomenon and precipitation in Mexico. *Geofísica Internacional* 49: 245-261. <https://doi.org/10.22201/igeof.00167169p.2010.49.4.132>
- Caso M, González-Abraham C, Ezcurra E. 2007. Divergent ecological effects of oceanographic anomalies on terrestrial ecosystems of the Mexican Pacific Coast. *Proceedings of the National Academy of Sciences* 104: 10530-10535. <https://doi.org/10.1073/pnas.0701862104>
- Cavazos T, Turrent C, Lettenmaier DP. 2008. Extreme precipitation trends associated with tropical cyclones in the core of the North American Monsoon. *Geophysical Research Letters* 35: L21703. <https://doi.org/10.1029/2008GL035832>
- Cruz-González A, Arteaga-Ramírez R, Sánchez-Cohen I, Soria-Ruiz J, Monterroso-Rivas AI. 2024. Impacts of climate change on corn production in Mexico. *Revista Mexicana de Ciencias Agrícolas* 15: e3327. <https://doi.org/10.29312/remexca.v15i1.3327>
- Douglas MW, Maddox RA, Howard K, Reyes S. 1993. The Mexican Monsoon. *Journal of Climate* 6: 1665-1677. [https://doi.org/10.1175/1520-0442\(1993\)006<1665:T-MM>2.0.CO;2](https://doi.org/10.1175/1520-0442(1993)006<1665:T-MM>2.0.CO;2)
- Félix-Burrueal RE, Larios E, González EJ, Búrquez A. 2021. Episodic recruitment in the saguaro cactus is driven by multidecadal periodicities. *Ecology* 102: e03458. <https://doi.org/10.1002/ecy.3458>
- Gochis DJ, Brito-Castillo L, Shuttleworth WJ. 2006. Hydroclimatology of the North American Monsoon region in Mexico. *Journal of Hydrology* 316: 53-70. <https://doi.org/10.1016/j.jhydrol.2005.04.021>
- Gutzler DS, Wood KM, Ritchie EA, Douglas AV, Lewis MD. 2013. Interannual variability of tropical cyclone activity along the Pacific coast of North America. *Atmósfera* 26: 149-162. [https://doi.org/10.1016/S0187-6236\(13\)71069-5](https://doi.org/10.1016/S0187-6236(13)71069-5)
- Houze RA Jr. 2012. Orographic effect on precipitating clouds. *Reviews of Geophysics* 50: RG1001. <https://doi.org/10.1029/2011RG000365>
- Hu Q and Feng S. 2002. Interannual rainfall variations in the North American summer monsoon region: 1900-98. *Journal of Climate* 15: 1189-1202. [https://doi.org/10.1175/1520-0442\(2002\)015<1189:IRVIT-N>2.0.CO;2](https://doi.org/10.1175/1520-0442(2002)015<1189:IRVIT-N>2.0.CO;2)
- Leite-Filho AT, Soares-Filho BS, Davis JL, Abrahão GB, Börner J. 2021. Deforestation reduces rainfall and agricultural revenues in the Brazilian Amazon. *Nature Communications* 12: 2591. <https://doi.org/10.1038/s41467-021-22840-7>
- Llanes-Cárdenas O, Norzagaray-Campo M, Gaxiola A, González-González GE. 2020. Regional precipitation teleconnected with PDO-AMO-ENSO in northern Mexico. *Theoretical and Applied Climatology* 140: 667-681. <https://doi.org/10.1007/s00704-019-03003-7>
- Magaña VO, Vázquez JL, Pérez JL, Pérez JB. 2003. Impact of El Niño on precipitation in Mexico. *Geofísica Internacional* 42: 313-330. <https://doi.org/10.22201/igeof.00167169p.2003.42.3.949>
- Mandujano S. 2006. Preliminary evidence of the importance of ENSO in modifying food availability for white-tailed deer in a Mexican tropical dry forest. *Biotropica* 38: 695-699. <https://doi.org/10.1111/j.1744-7429.2006.00184.x>
- Muñoz-Arriola F, Avissar R, Zhu Ch, Lettenmaier DP. 2009. Sensitivity of the water resources of Rio Yaqui Basin, Mexico, to agriculture extensification under multiscale climate conditions. *Water Resources Research* 45: W00A20. <https://doi.org/10.1029/2007WR006783>
- Nesbitt SW, Gochis DJ, Lang TJ. 2008. The diurnal cycle of clouds and precipitation along the Sierra Madre Occidental observed during NAME-2004: Implications for warm season precipitation estimation in complex terrain. *Journal of Hydrometeorology* 9: 728-743. <http://doi.org/10.1175/2008JHM939.1>

- Notaro M, Gutzler D. 2012. Simulated impact of vegetation on climate across the North American monsoon in CCSM3.5. *Climate Dynamics* 38: 795-814. <https://doi.org/10.1007/s00382-010-0990-0>
- Oliver JE. 1980. Monthly precipitation distribution: A comparative index. *The Professional Geographer* 32(3): 300-309. <https://doi.org/10.1111/j.0033-0124.1980.00300.x>
- ONI. n.d. Historical El Niño/La Niña episodes (1950-present). Cold & warm episodes by season. Climate Prediction Center, National Weather Service, NOAA. Available at https://origin.cpc.ncep.noaa.gov/products/analysis_monitoring/ensostuff/ONI_v5.php (accessed 30 November 2023)
- Pompa-García M, Miranda-Aragón L, Aguirre-Salado CA. 2015. Tree growth response to ENSO in Durango, Mexico. *International Journal of Biometeorology* 59: 89-97. <https://doi.org/10.1007/s00484-014-0828-2>
- Rodríguez-Morales U, Corona-Vásquez B, Prieto-González, Martínez-Austria P. 2023. Influence of the AMO and its modulation of the ENSO effects on summer precipitation in Mexican coastal regions. *Water Practice & Technology* 18: 304-319. <https://doi.org/10.2166/wpt.2023.015>
- Rowe AK, Rutledge SA, Lang TJ, Ciesielski PE, Saleeby SM. 2008. Elevation-dependent trends in precipitation observed during NAME. *Monthly Weather Review* 136: 4962-4979. <https://doi.org/10.1175/2008MWR2397.1>
- Salinas-Zavala CA, Douglas AV, Díaz HF. 2002. Interannual variability of NDVI in northwest Mexico. Associated climatic mechanisms and ecological implications. *Remote Sensing of Environment* 82: 417-430. [https://doi.org/10.1016/S0034-4257\(02\)00057-3](https://doi.org/10.1016/S0034-4257(02)00057-3)
- Taschetto AS, Ummenhofer CC, Stuecker MF, Dommenget D, Ashok K, Rodrigues RR, Yeh S-W. 2020. ENSO atmospheric teleconnections. In: *El Niño Southern Oscillation in a changing climate*, 1st ed. (McPhaden MJ, Santoso A, Cai W, Eds.). *Geophysical Monograph* 253, 309-335. <https://doi.org/10.1002/9781119548164.ch14>
- Vera C, Higgins W, Amador J, Ambrizzi T, Garreaud R, Gochis D, Gutzler D, Lettenmaier D, Marengo J, Mechoso CR, Nogues-Paegle J, Silva-Dias PL, Zhang C. 2006. Towards a unified view of the North American Monsoon systems. *Journal of Climate* 19: 4977-5000. <https://doi.org/10.1175/JCLI3896.1>
- Verduzco VS, Garatuza-Payán J, Yépez EA, Watts CJ, Rodríguez JC, Robles-Morua A, Vivoni ER. 2015. Variations of net ecosystem production due to seasonal precipitation differences in a tropical dry forest of northwest Mexico. *Journal of Geophysical Research: Biogeosciences* 120: 2081-2094. <https://doi.org/10.1002/2015JG003119>
- Zermeño-Díaz DM, Gómez-Mendoza L. 2023. The influence of ENSO during spring over northwestern Mexico. 2023. *International Journal of Climatology* 43: 6420-6433. <https://doi.org/10.1002/joc.8212>
- Zhao P, Wang B, Liu J, Zhou X, Chen J, Nan S, Liu G, Xiao D. 2016. Summer precipitation anomalies in Asia and North America induced by Eurasian non-monsoonal land heating versus ENSO. *Scientific Reports* 6: 21346. <https://doi.org/10.1038/srep21346>